19e Journées de l'Hydrodynamique
26 – 28 novembre 2024, Nantes

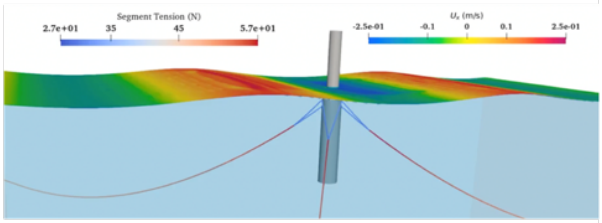


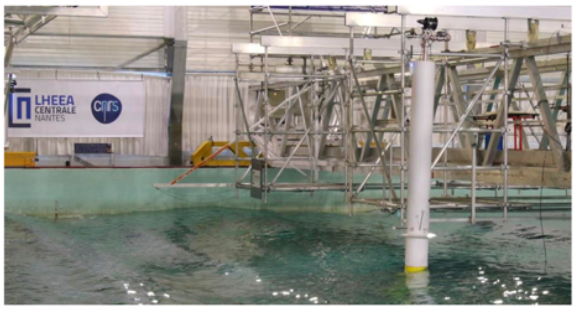


# *VERTICAL AXIS TIDAL TURBINE BEHAVIOUR IN A NON-UNIFORM VELOCITY PROFILE*

**R. LINANT[1,2], G. GERMAIN[1], J-V. FACQ[1], C. PENISSON[2],G. MAURICE[2]**
*robin.linant@ifremer.fr ; gregory.germain@ifremer.fr*

[1]Ifremer, Marine Hydrodynamics Laboratory, Boulogne-sur-mer
[2]HydroQuest SAS, Meylan

## Résumé

Les retours positifs du test d'un démonstrateur marin d'une puissance unitaire de 1MW sur le site de Paimpol Bréhat permettent à l'entreprise HydroQuest de s'affirmer sur le marché de l'hydrolien avec une technologie d'hydrolienne à axe vertical (VATT). Dans la perspective d'implanter 6 machines de nouvelle génération au Raz Blanchard (projet FloWatt), il est essentiel d'améliorer les outils numériques et expérimentaux pour prédire le comportement de ces machines à l'échelle 1. Ainsi, des essais en laboratoire sur une maquette d'hydrolienne à double axe vertical bi-rotors contrarotatifs à échelle 1/20 sont réalisés afin d'étudier son comportement en présence d'un gradient vertical de vitesse. Les résultats montrent que l'écoulement cisaillé est responsable d'une asymétrie de chargement entre le rotor supérieur et inférieur, avec une production de couple moins importante pour le rotor inférieur et d'une baisse de performance de la turbine. L'étude du sillage montre quant à elle que le champ proche est modifié par l'écoulement cisaillé.

## Summary

The positive feedback from the test of a 1MW marine demonstrator at the Paimpol Bréhat test site has enabled HydroQuest to assert itself on the tidal turbine market with vertical axis tidal turbine (VATT) technology. Intending to install 6 new-generation machines at the Alderney Race (FloWatt project), it is essential to improve numerical and experimental tools to predict the behaviour of these machines at full scale. Thus, Laboratory tests on a 1/20-scale model of a twin-rotor counter-rotating vertical-axis tidal turbine are carried out to study its behaviour in the presence of a vertical velocity gradient. The results show that the sheared flow is responsible for asymmetric loading between the upper and lower rotors, with the lower rotor producing less torque and reducing turbine performance. The wake study shows that the near-field is modified by the sheared flow.

# I – Introduction

Facing growing energy demand and climate challenges, research and development associated with tidal energy converters (TECs) have expanded considerably over the past decade. This renewable energy source has the advantage of being predictable, with a high potential [5]. A revolutionary project known as Flowatt is currently being developed and will see its completion in the next few years. Six turbines will be installed in the Alderney Race. In this area, the tidal turbines will be subject to complex flow conditions, as it is known that tidal currents are spatially and temporally variable and are influenced by the flow direction, presence of waves, sheared velocity profile and in some cases a combination of all these phenomena [11, 10]. Numerous studies have focused on the effect of flow direction and wave-current-structure interaction on the behaviour of machines [8, 12].

However, the effect of the sheared velocity profile has mainly been studied on Horizontal Axis Tidal Turbines (HATTs). [6] analysed the impact of vertical shear velocity profiles on both the estimation of tidal turbine performance and blade loading variation. They concluded that the inlet velocity profile does not influence average turbine performance, but that blade load variations are cyclic. From numerical studies, [2] shown that the velocity shear is responsible for 12% reduction of the power output and increases the blade deformation of a HATT. [4] has highlighted the importance of the shear flow rate being directly related to load fluctuations.

Although HATTs are popular, Vertical Axis Tidal Turbines (VATTs) are also interesting for capturing tidal energy. However, as the authors know, the effect of the sheared velocity profile on the behaviour of VATTs has not yet been fully established. Only a few studies consider this effect in particular as the one carried out by Moreau [9] on a ducted twin vertical axis tidal turbine. They concluded that, for this kind of turbine, the current shear increases the power fluctuations by 35% compared to uniform flow.

The new generation of HydroQuest turbines being unducted, we have to resume this kind of studies in order to identify the effect of removing the fairing. Section II first describes the scale-model and the experimental set-up carried out in the Ifremer's wave and current flume tank. Section III reports on the velocity profile effect on the global and stage-by-stage performance of the 2-VATT. The dynamic of the wake close to the turbine is also analysed using 3C-LDV measurements. Finally, section V summarised the results.

# II – Materials and methods

## II – 1 Turbine model

The 2-VATT studied is a 1:20 scale model of the full-scale 2.5 MW machines developed for the FloWatt project (Fig. 1 (left)). Two independent counter-rotating vertical axis rotor columns, composed of two levels of Darrieus-type rotors with a 60° phase difference between them, allow to capture the flow kinetic energy. Each rotor of radius $R = 0.235$m is made of N=3 blades with NACA 0022 profiles, such that the blade height ($H_{blade}$) is 0.315m and the chord ($c$) is 0.063m. The turbine height is defined as the distance between the top and bottom horizontal plates such that $h_m = 0.83$m. The model has a height of $H_{struc} = 1.01$m and a width of $w_m = 1.27$m between the two columns. The turbine is fixed on a tripod base through a 6-component load cell (SIXAXES 1.5 kN). The tripod structure comprises three ballasted arms linked to the anchor base. The electronic systems are installed in two watertight blocks located under the two columns. Each block comprises a $Maxon\ RE50$ 200W motor equipped with a 1/26th gear reducer and a speed

encoder. A *Scaime* $DR2112-W$ torque meter with a relative angular position encoder also composes the blocks. The motors are piloted using remote $EPOS2$ servo-controllers in constant speed mode.

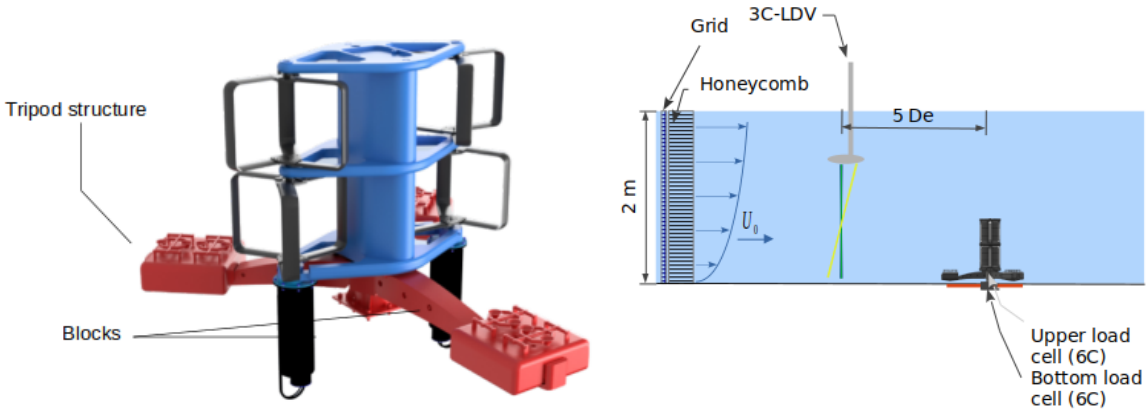


Figure 1: Schematic view of the twin counter-rotating VATT model on the tripod base (left). Scheme of the experimental setup in the Ifremer's wave and current flume tank (right).

For this study, two configurations (noted P1 and P2) were tested to assess the impact of the direction of the turbine compared with the incident flow (Fig. 2). For case P1, the counter-rotating rotor blades push the flow at the 2-VATT central pillar and the incident flow encounters a single base pile, aligned with the central pillar of the turbine. For case P2, the rotor blades suck the flow at the centre of the 2-VATT and the upstream flow encounters two base piles, each aligned with the outer side of the circles swept by the rotors.

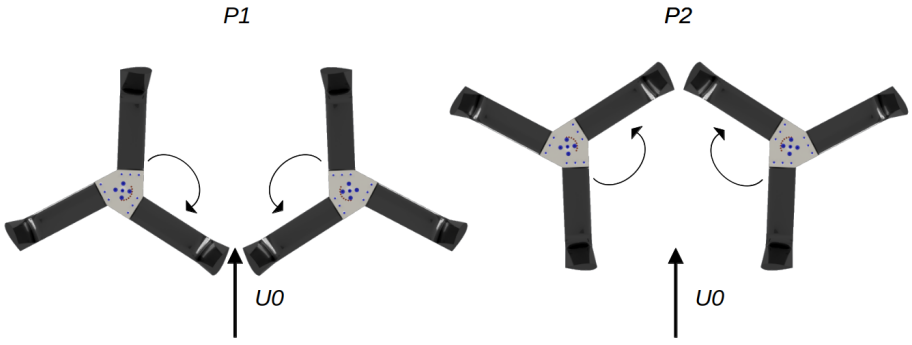


Figure 2: Schematic view of the two rotational directions of the counter-rotating rotors.

## II – 2 Experimental setup

To study the impact of the velocity gradient on the 2-VATT behaviour, tests have been carried out in the Ifremer wave and current flume tank in Boulogne-sur-Mer, France. The working section is $l_{wat}$ = 18m long × $w_{wat}$ = 4m wide × $h_{wat}$ = 2m deep. Consequently, the blockage ratio ($b = \frac{(HW)_{struc}}{(hw)_{water}}$), is about 17% with the tripod base. According to the literature, the surface blockage ratio influences power output and turbine near wake characteristics [3].

The orthogonal coordinates system considered is such that the x-coordinate points in the direction of the current and the y-coordinate faces the wall, with both origins located at the model's centre. Finally, the z-coordinate is oriented towards the surface, with its origin on the tank floor.

The incoming flow ($U_0$, $V_0$, $W_0$) is assumed to be constant and steady. The three instantaneous velocity components are denoted ($U$, $V$, $W$) along the ($x$, $y$, $z$) directions respectively. The turbulence rate in the tank is controlled by adding a grid and a honeycomb at the inlet (Fig. 1 (right)). The grid is generally homogeneous to generate a uniform velocity profile. For this study, a special system is used to generate a sheared velocity profile, which consists of an arrangement of grids of different porosity depending on the depth of water [7].

## II – 3 Data acquisition and processing

To correctly address the performance of the 2-VATT, the current velocity is measured using a *Dantec* 3-Component Laser Doppler Velocimeter (3C-LDV) in non-coincident mode, such that each velocity component is measured independently of the others. The tank is seeded with spherical silver-coated glass micro-particles with a diameter of $10\mu m$. This probe measures the flow velocity in the three spatial directions ($x$, $y$, $z$). The probe is placed at $x/De$ = -5, with $De = \sqrt{\frac{4S_{ref}}{\pi}}$ the equivalent diameter defined from the projected capture area of the turbine $S_{ref} = h_m \times w_m$. Vertical profiles are established in the centre of the empty tank to extract a reference velocity (noted $U_0$), defined as the average streamwise velocity below the capture area (Fig. 3 (left)). Thus, $U_0$ is taken to be equal to 0.99 (resp. 0.93) $\pm$ 0.01 m.s$^{-1}$ in the uniform (resp. sheared) flow. Synchronously with the 3C-LDV, the torque ($Q$), the rotational speed ($\omega$) of each rotor

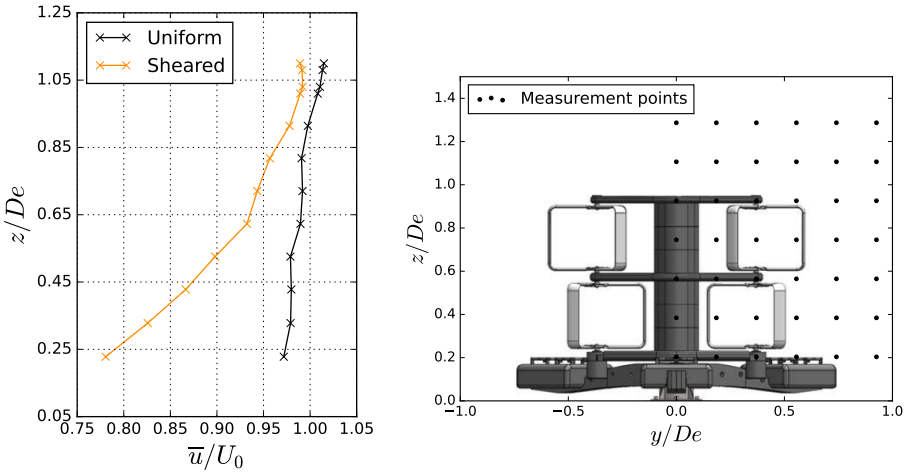


Figure 3: Vertical profiles of the mean axial velocity $\overline{u}/U_0$ with the 3C-LDV probe at the centre of the tank without the turbine (left). Mesh used for velocity measurements by the 3C-LDV (right).

column and the two load cell signals are acquired using *National Instruments PXI* and *LabView* systems. The acquisitions last 3 minutes to guarantee the time convergence of the mean and standard deviation of the signals. Each run is sampled at a frequency of 128 Hz. The performance of the 2-VATT is studied through its power coefficient ($C_P$) in

relation to the tip speed ratio ($TSR$), defined in Eq. 1 to 2.

$$C_P = \frac{P}{0.5\rho S_{ref} U_0^3} \tag{1}$$

$$C_Q = \frac{P}{0.5\rho \frac{S_{ref}}{2} R U_0^2};\ TSR = \frac{\omega R}{U_0} \tag{2}$$

The phase average of the torque coefficient ($C_Q$, Eq. 2) is evaluated with its angular distribution. The instantaneous phase is computed by Hilbert transform of the torque filtered at the rotational frequency ± 0.005 Hz. Thus, the angular position is relative and cannot be compared between graphs.

In addition to performance, the wake is also analysed using the 3C-LDV probe. The turbine is set to its optimal operating point ($TSR = 2.2$). As the symmetry of the velocity profiles was verified behind the two rotor columns, only the velocities of the right half of the model were measured (Fig. 3). The velocity maps presented below are based on linear interpolation between each measurement point.

# III – Global behaviour of the unducted 2-VATT

## III – 1 Full machine

Fig. 4 displays the power coefficients of the turbine in the uniform and sheared velocity profiles for P1 and P2. The results show that the input velocity profile interferes slightly with the machine's behaviour by reducing the output power. Indeed, at the optimal

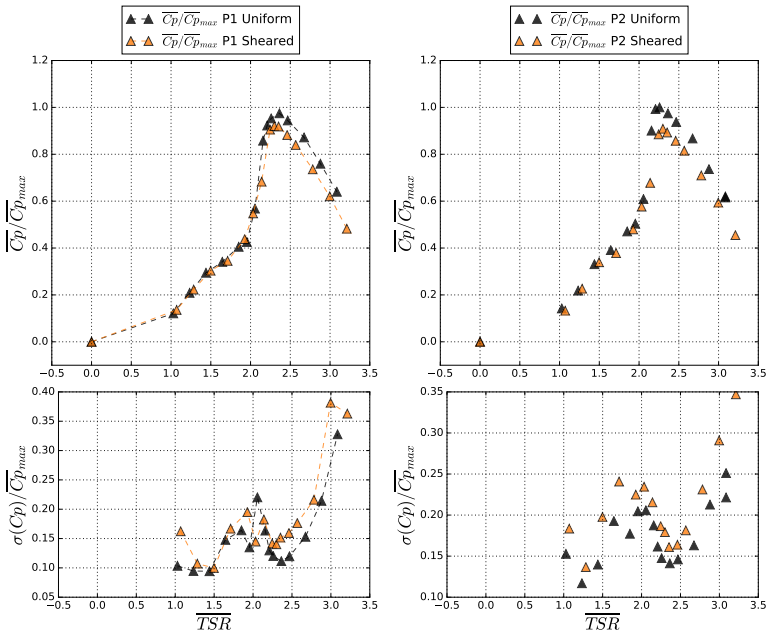


Figure 4: Average (top) and standard deviation (bottom) of the power coefficient in P1 (left) and P2 (right) with uniform and shear conditions. The curves are normalised by the maximal average value in "P2 Uniform".

tip speed ratio, the sheared velocity profile reduces the average power coefficient by 6% and 9% in P1 and P2 respectively. The evaluation of power fluctuations shows that the nature of the incident flow strongly affects the standard deviation. A significant increase is observed with the sheared flow of the order of 20% and 18% in P1 and P2.

To go further, the angular distribution of the torque coefficient is plotted in Fig. 5. By comparing the two flow configurations it can be observed that P1 is less sensitive than the P2 configuration by the presence of the vertical sheared profile. Overall, the angular torque distribution is similar in P1 uniform and P1 sheared, with 3 peaks and troughs. The distribution is such that two peaks or troughs have a phase difference of 120°, similar to the geometric phase difference between two rotor blades. However, in P1 uniform, the

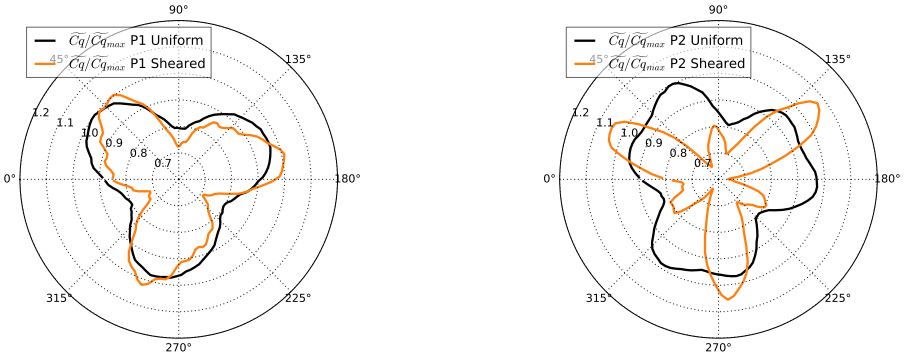


Figure 5: Phase-averaged angular distribution of the torque of one column in P1 (left) and P2 (right) at the optimal tip speed ratio for the uniform and sheared flow cases. For the Pn configuration, the maximal phase average in "Pn Uniform" (with n = 1, 2) normalises the angular distribution

energy production phase (i.e. where the torque reach is maximum) takes place over a phase range of 60°, corresponding to the phase shift between the upper and lower rotors of a column, whereas in P1 sheared the maximum torque is reached over a shorter range. This means that in P1 uniform, the two rotors of a column produce equally, while in P1 sheared, one of the two rotors produces more than the other. This is particularly true for P2, where the sheared flow shows six torque peaks corresponding to the contribution of each blade. The distribution is unevenly distributed with 3 high-intensity peaks and 3 low-intensity peaks. Thus, an asymmetry in torque production between the upper and lower rotors of the column is observed, with a difference of around 25%.

## III – 2 Single-stage rotors

To look at the effect of shear flow on the rotors, we studied the torque distribution stage by stage. To do this, mechanical couplings have replaced the rotors of one stage to allow connection to the column.

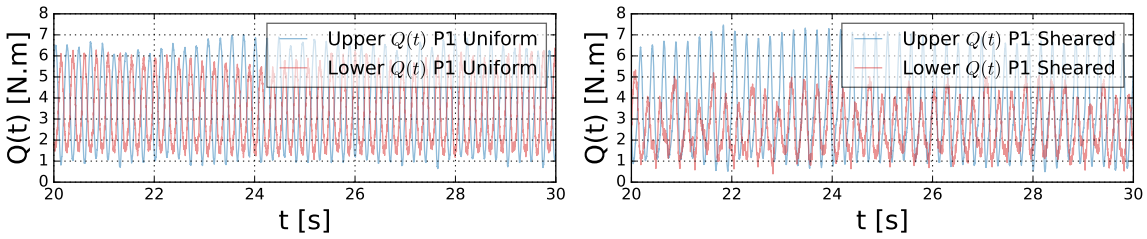


Figure 6: Time-averaged torque of the upper and lower rotors of the column in the P1 configuration for uniform (left) and sheared (right) flow.

Fig. 6 displays the time average of the torque of the upper and lower rotors of the column in the P1 configuration for uniform and sheared flow. Firstly, with the uniform vertical profile, the upper and lower rotors produce almost equally, with a slight difference of around 6%. Overall, the two rotors capture identical energy from the incident flow. On the contrary, the sheared vertical profile shows that the upper rotor produces 1.4 times more than the lower rotor. In other words, the velocity gradient imposes a different operating condition on the two rotors in the column.

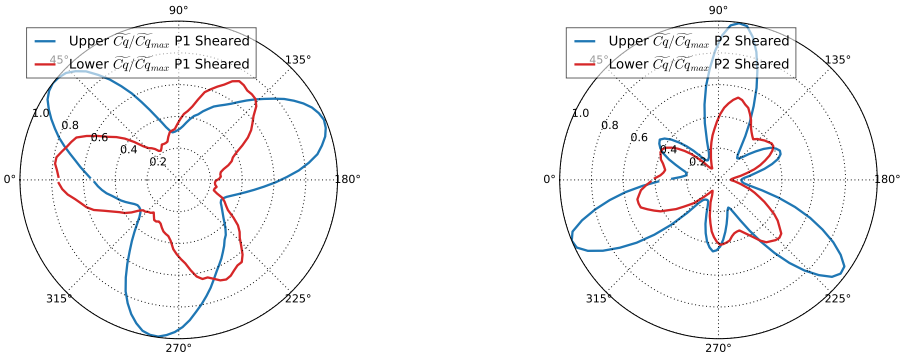


Figure 7: Phase-averaged angular distribution of the torque of the upper and lower rotors in P1 (left) and P2 (right) sheared at the optimal tip speed ratio.

To sum up, Fig. 7 presents the phase average of the angular distribution and the Fourier transform of the torque of the upper and lower rotor in P1 and P2 sheared conditions. For P1, the averaged $C_Q$ is unequal between the upper and lower rotor of the column. Although the rose shapes have a similar pattern with 3 peaks and troughs, the upper rotor has a maximum phase-averaged torque 20% higher than the lower rotor. The asymmetric distribution of $Q(t)$ is also visible in P2 but the shape of the roses is quite different. Indeed, it can be seen that the rotor alone, consisting of 3 blades, generates 6 torque peaks as if the column consisted of two levels of rotors. This can be explained by the initial pitch of a blade, which is not zero. So each rotor blade produces in two regions. The highest production is for azimuth angles $\in [0°;180°]$ (i.e. in the upstream region of the rotor) and a small amount is produced in the downstream region of the rotor represented by the azimuth angles $\in [180°;360°]$ [1]. Thus, The angular distribution shows 3 peaks of high intensity, corresponding to production in the upstream part, and 3 peaks of low intensity, corresponding to production in the downstream part. If we consider only the high-intensity peaks (i.e. maximum torque production) a difference of 47% is noticeable between the upper rotor and the lower rotor. Those results reveal that the behaviour of the 2-VATT is affected by the presence of the vertical velocity profile in the two flow directions and can lead to significant structural fatigue.

## IV – Aligned sheared flow effect on the wake

In addition to the turbine's performance, the focus is now done on the development of the 2-VATT's wake to characterise its impact on its environment. In the remainder of this study, we make a focus on case P1.

Fig. 8 displays the field of the near mean u-velocities contours with superimposition of arrow fields of the mean transverse velocities $(\overline{v}, \overline{w})/U_0$. The flow dynamics downstream of the turbine are compared for the two incident velocity profiles. The maps reveal that the

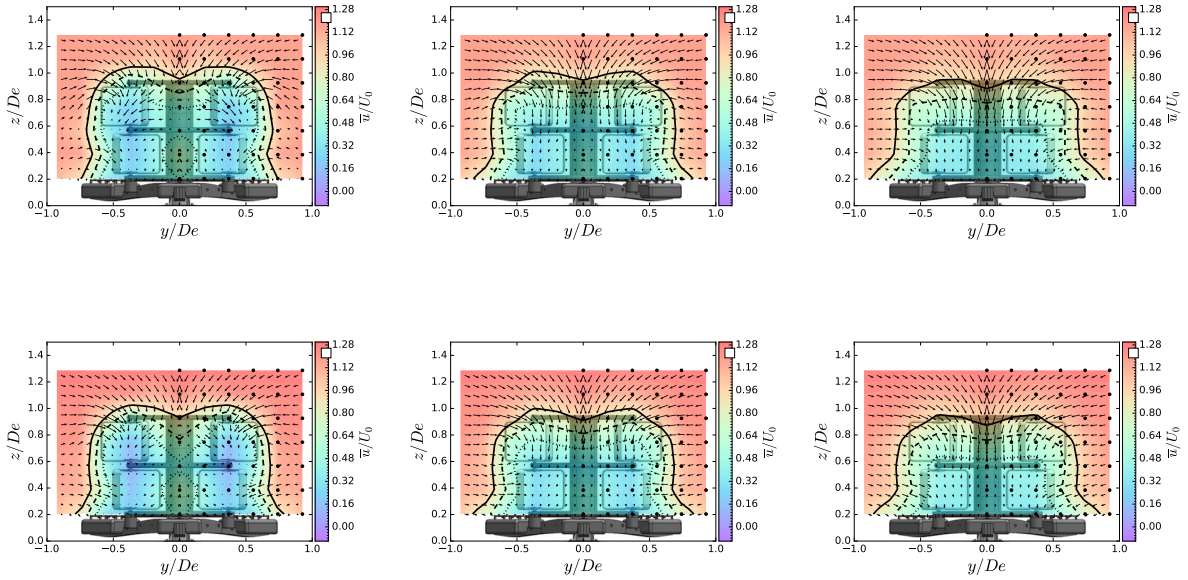


Figure 8: Contours of the mean streamwise velocity in $(y, z)$ planes, with the superimposition of the arrow field of the mean transverse velocities $(\overline{v}, \overline{w})/U_0$ in uniform flow (top) and sheared flow (bottom) for three different downstream locations. The solid, dashed and dotted black lines are iso-contours of $\overline{u}/U_0 = 0.9$, 0.7 and 0.5 respectively.

incoming velocity barely affected the geometry of the near wake of the unducted 2-VATT. Two swirl structures are developed behind each rotor column and around the $x$-axis for both conditions. They are created to contribute to the mixing between the ambient flow and the wake generated by the presence of the turbine.

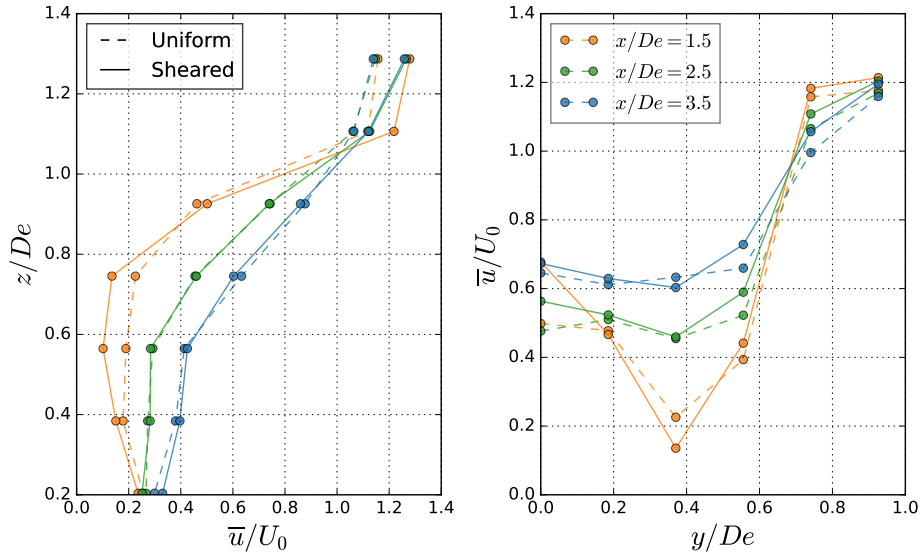


Figure 9: Vertical (left) and horizontal (right) profiles (at $y/De = 0.37$ and $z/De = 0.74$ respectively) of the average streamwise component of the normalised velocity $\overline{u}/U_0$ for different x-positions in uniform and shear flow.

In addition to the maps, the vertical profiles plotted in Fig. 9 present the evolution of the average streamwise velocity $\overline{u}/U_0$ behind the middle of the rotor column at different positions downstream of the turbine in uniform flow and sheared flow. For both flow conditions, the velocity deficit behind the rotor column, defined as the area in which $\overline{u}/U_0 < 0.5$, is more important at $x/De = 1.5$. The presence of the vertical sheared profile has an even greater impact on the turbine wake because the velocity deficit at this distance $x/De$ is increased by 42% compared with the uniform flow just behind the middle of the upper rotor. Further downstream of the model (i.e. $x/De = 2.5$ and 3.5), the evolution of the wake is similar between laminar and sheared flow. Moreover, we can also see that beyond the position $z/De = 1.0$, the sheared velocity profile imposes an overspeed 6% stronger than the uniform flow. The same trend is observed with the horizontal profile just behind the middle of the upper rotor, which shows a 43% velocity deficit stronger with the sheared flow on the measurement behind the rotor at $x/De = 1.5$. As for the vertical profiles, the horizontal profiles are similar between the two kinds of flow for the distances $x/De = 2.5$ and $x/De = 3.5$.

Therefore, additional measurements in the far wake of the turbine need to be undertaken to gain a better understanding of the impact of the incident flow on wake resorption.

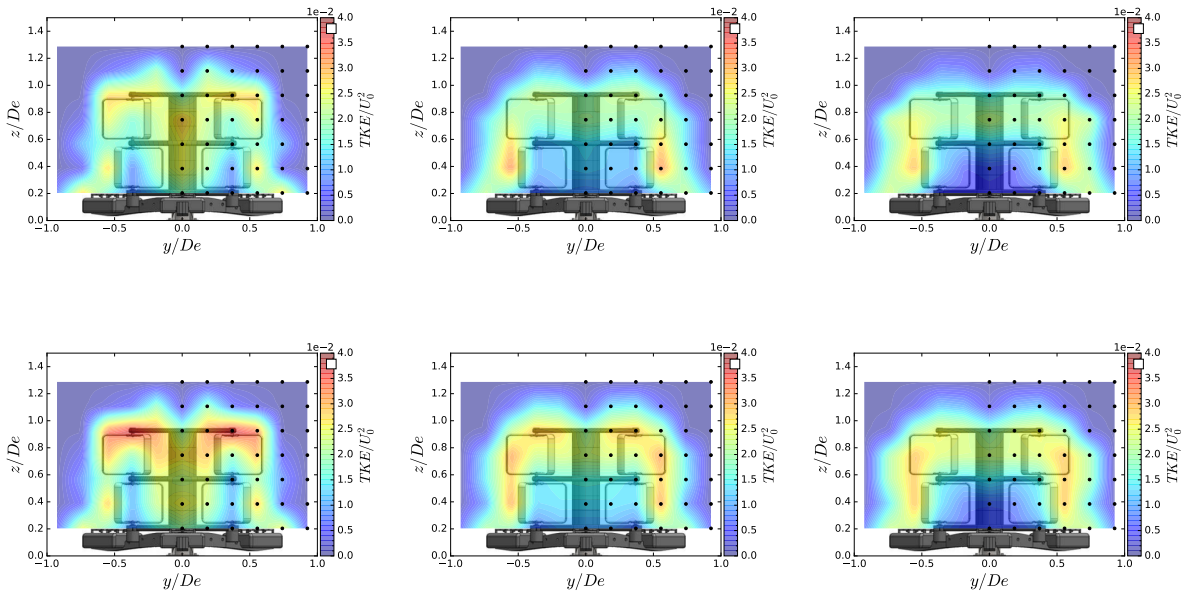


$x/De = 1.5$ $x/De = 2.5$ $x/De = 3.5$

Figure 10: Contours of the turbulent kinetic energy ($TKE$) in $(y, z)$ planes, computed on $u$, $v$ and $w$ in uniform flow (top) and sheared flow (bottom) for three different downstream locations.

To sum up, the 3D turbulent kinetic energy $TKE = 0.5(\sigma(u)^2 + \sigma(v)^2 + \sigma(w)^2)$ is plotted in Fig. 10. Overall, the plans show that the dynamics behind the turbine follow more or less the same trend. In both cases, the kinetic energy is mainly located at the top plate of the turbine and the rotor tips. This is mainly due to the flow bypassing the model and the vortices being released at the blade tip [8]. By comparing the two flow conditions, the kinetic energy is higher with the presence of the sheared velocity profile. Indeed, in the sheared flow, the maximal $TKE$ is 27 % higher than in the uniform flow at $x/De = 1.5$. Fig. 11 displays the surface average of the mean TKE over the region

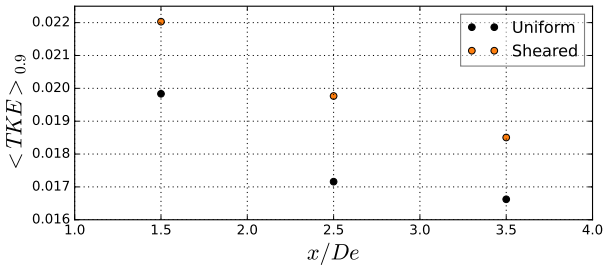


Figure 11: Evolution of the mean turbulent kinetic energy with uniform and sheared flow (surface average over the region delimited by $0.9U_0$).

delimited by $0.9U_0$ for different streamwise positions. This quantity reveals the strength of the kinetic energy in the entire turbine wake zone. It is observed that the general dynamics are ensured by the nature of the incoming flow. The sheared flow shows a stronger kinetic energy density over all the downstream distances studied. Overall, the presence of the vertical sheared profile results in an increase of roughly 10% in velocity fluctuations within the wake of the model. These results show that the dissipation of kinetic energy is quicker for uniform flow.

## V – Conclusions

The literature usually provides answers about the behaviour of tidal turbines under idealised conditions. In reality, turbines are confronted with sheared velocity profiles due to the bathymetric effects. This paper aims to clarify the impact of the vertical velocity gradient on the hydrodynamic behaviour of an unducted twin vertical axis tidal turbine (2-VATT).

The results show that the average power coefficient is slightly affected by the presence of the sheared flow. However, the standard deviation considerably increases by around 20% with the vertical sheared profile. The torque angular distribution is also modified with the upstream flow shear, revealing an asymmetry between the upper and lower rotors.

Secondly, the stage-by-stage analysis shows in more detail the asymmetry of the upper and lower rotor of the 2-VATT column. While torque production is almost the same between the upper and lower rotors for uniform flow, the time-averaged torque in the non-uniform velocity profile shows that the torque is 1.4 times higher for the machine's upper rotors. Therefore, the upper and lower rotors work under different operating conditions because of the difference in incident velocity imposed by the sheared flow.

Finally, regarding the wake of the unducted 2-VATT, the near wake shows that the velocity profile is responsible for an increase in the velocity deficit in the field very close to the turbine. Beyond, the two flows reveal large swirls around the $x$-axis. Looking at the turbulent kinetic energy, the velocity gradient imposes a higher $TKE$ in the near wake of the turbine. Thus, The flow bypassing is more pronounced in the presence of a non-uniform velocity profile. The study also reveals that the $TKE$ is dissipated less rapidly with the incoming sheared flow.

Therefore, for the next series of tests, a study of the far wake should be carried out to gain a deeper understanding of wake dynamics and the impact of the sheared velocity profile on the unducted 2-VATT's wake development.

## Acknowledgements

The authors acknowledge Y. Saouli, B. Gaurier and B. Gomez for their help during the experiments.

## References

[1] P.-L. Delafin, F. Deniset, J. Astolfi, and F. Hauville. Performance Improvement of a Darrieus Tidal Turbine with Active Variable Pitch. *Energies*, 14:667, Jan. 2021.

[2] N. Hafeez, S. Badshah, M. Badshah, and S. Khalil. Effect of velocity shear on the performance and structural response of a small-scale horizontal axis tidal turbine. *Marine Systems & Ocean Technology*, 14, July 2019.

[3] A. Hunt, A. Athair, O. Williams, and B. Polagye. *Experimental validation of a linear momentum and bluff-body model for high-blockage cross-flow turbine arrays.* Aug. 2024.

[4] S. Ke, W. Wen-Quan, and Y. Yan. The hydrodynamic performance of a tidal-stream turbine in shear flow. *Ocean Engineering*, 199:107035, Mar. 2020.

[5] X. Liu, Z. Chen, Y. Si, P. Qian, H. Wu, L. Cui, and D. Zhang. A review of tidal current energy resource assessment in china. *Renewable and Sustainable Energy Reviews*, 145:111012, July 2021.

[6] M. Magnier, N. Delette, P. Druault, B. Gaurier, and G. Germain. Experimental study of the shear flow effect on tidal turbine blade loading variation. *Renewable Energy*, 193:744–757, June 2022.

[7] M. Magnier, G. Germain, B. Gaurier, P. Druault, B. Gaurier, and P. Druault. Velocity profile effects on a bottom-mounted square cylinder wake and load variations. Sept. 2021.

[8] M. Moreau, G. Germain, J.-V. Facq, G. Maurice, and C. Derveaux. Experimental study of two opposed flow directions effect on a ducted twin vertical axis tidal turbine. 2023.

[9] M. Moreau, G. Germain, and G. Maurice. Misaligned sheared flow effects on a ducted twin vertical axis tidal turbine. *Applied Ocean Research*, 138:103626, Sept. 2023.

[10] H. Mullings, S. Draycott, J. Thiébot, S. Guillou, P. Mercier, J. Hardwick, E. Mackay, P. Thies, and T. Stallard. Evaluation of Model Predictions of the Unsteady Tidal Stream Resource and Turbine Fatigue Loads Relative to Multi-Point Flow Measurements at Raz Blanchard. *Energies*, 16(20):7057, Jan. 2023.

[11] M. Piano, S. P. Neill, M. J. Lewis, P. E. Robins, M. R. Hashemi, A. G. Davies, S. L. Ward, and M. J. Roberts. Tidal stream resource assessment uncertainty due to flow asymmetry and turbine yaw misalignment. *Renewable Energy*, 114:1363–1375, Dec. 2017.

[12] W. Zang, Y. Zheng, Y. Zhang, J. Zhang, and E. Fernandez-Rodriguez. Experiments on the mean and integral characteristics of tidal turbine wake in the linear waves propagating with the current. *Ocean Engineering*, 173:1–11, 2019.